



Science Arts & Métiers (SAM)

is an open access repository that collects the work of Arts et Métiers Institute of Technology researchers and makes it freely available over the web where possible.

This is an author-deposited version published in: <https://sam.ensam.eu>
Handle ID: <http://hdl.handle.net/10985/19686>

To cite this version :

Linda AISSANI, Akram ALHUSSEIN, Lamia RADJEHI, Issam LAKDHAR, Elia ZGHEIB, Corinne NOUVEAU - Evolution of microstructure, mechanical and tribological properties of vanadium carbonitride coatings sputtered at different nitrogen partial pressures - Surface and Coatings Technology - Vol. 374, p.531-540 - 2019

Any correspondence concerning this service should be sent to the repository

Administrator : scienceouverte@ensam.eu



Evolution of microstructure, mechanical and tribological properties of vanadium carbonitride coatings sputtered at different nitrogen partial pressures

Linda Aissani^{a,b}, Akram Alhussein^{c,*}, Corinne Nouveau^d, Lamia Radjehi^a, Issam Lakdhar^c, Elia Zgheib^c

^a Mater Science Department, ABBES Laghrour-Khenchela University, P.O. Box 1252, 40004, Algeria

^b Materials and Tribology Group, Laboratory of Foundry, Annaba University BO, 12 CP 23000, Algeria

^c ICD-LASMIS, Université de Troyes, CNRS, Antenne de Nogent, Pôle Technologique Sud Champagne, 26 Rue Lavoisier, 52800 Nogent, France

^d Arts et Metiers ParisTech, Laboratoire Bourguignon des Matériaux et Procédés, Rue Porte de Paris, 71250 Cluny, France

ARTICLE INFO

Keywords:

V-C-N thin films

Magnetron sputtering

Nitrogen pressure

Microstructure

Wear

Mechanical properties

ABSTRACT

Vanadium carbide coatings were deposited by R.F. reactive magnetron sputtering at different nitrogen partial pressures. The structures and the mechanical and tribological behaviour of these coatings were studied.

By using a combined approach of EDS and WDS, it has been shown that increasing nitrogen concentration from 0 to 27 at.% led to decrease the carbon content from 48.50 to 30.50 at.%. All coatings exhibited a dominant fcc-VC structure with additional fractions of vanadium nitrides, as determined by XRD. Nanoindentation measurements showed that the highest hardness of 26.1 GPa was obtained for the coating with a (N + C) / (V) ratio equal to 1.44. The transition in brittleness-ductile failure mode was noticed with increasing nitrogen content. This adhesive feature can prevent phase separation and improves the wear resistance of the coatings. Moreover, the nitrogen partial pressure showed a significant influence on the friction coefficient because of film density and residual stress effects.

1. Introduction

In the last few years, transition-metal carbides and nitrides have attracted much attention for technological purposes. They are extremely hard, having high melting points, good thermal conductivity, and good corrosion and wear resistance [1–3]. Among them, vanadium nitrides are very well-known materials widely applied as hard and wear resistant protective coatings for cutting tools or other components [4]. The addition of nitrogen to vanadium enhances mechanical and tribological properties, and significantly increases oxidation resistance, which is due to the formation of a dense fcc-VN phase [5]. Sarakinos reported the influence of nitrogen on the microstructure–property of reactive magnetron sputtered V–N films [6,7].

Vanadium carbides present a potential for industrial applications due to their excellent properties at high temperatures, such as good wear resistance and high hardness, attributed to the very fine grain dispersion in thin films [8]. Oliveira et al. [9] have reported the influence of carbon content on the mechanical properties of vanadium carbide coatings deposited by the thermo-reactive diffusion method

[9]. Also, Wu et al. [10] studied the effect of carbon content on the mechanical properties and electronic structure of various vanadium carbides. Until now, previous studies have reported the elaboration of vanadium carbides by different methods such as: pulsed laser deposition, magnetron sputtering and electron beam deposition [11–13].

Despite the vast application potential of vanadium carbide, its structural applications are limited by its brittleness, which has hindered its use in contrast to other transition-metal carbides [9,10,14]. This is especially due to the excessive amorphous carbon in the coatings that does not allow the dislocations to move and consequently a rapid fracture in the film takes place along the grain boundaries [15]. Therefore, several studies have been proposed to improve the toughness of vanadium carbide films based on their composition and microstructure by the introduction of nitrogen atoms into the V–C film structure. According to Khyzhun et al., the introduction of nitrogen into the carbides system has been shown to be very promising for the achievement of different properties such as wear resistance, residual stresses and hardness [16]. In fact, V-C-N coatings were reported to possess different properties in comparison to coatings based on the

* Corresponding author.

E-mail address: akram.alhussein@utt.fr (A. Alhussein).

Table 1

Electrical power and voltage applied to the vanadium and carbon targets and the chemical composition of the VC and V-C-N films deposited at 0.4 Pa during 120 min.

| Coatings | PN ₂ | V target | | C target | | Chemical composition (at.%) | | | | |
|----------|-----------------|----------|-------|----------|-------|-----------------------------|------|------|-----|---------|
| | | P(W) | U(-V) | P(W) | U(-V) | N | V | C | O | N + C/V |
| VC | 0.00 | | | | | 0 | 50.0 | 48.5 | 1.5 | 0.95 |
| | 0.02 | | | | | 6.7 | 47.0 | 45.0 | 1.3 | 1.10 |
| | 0.04 | | | | | 12.1 | 44.0 | 40.5 | 3.4 | 1.18 |
| V-C-N | 0.06 | 550 | 900 | 150 | 300 | 18.0 | 41.0 | 38.8 | 2.2 | 1.38 |
| | 0.08 | | | | | 22.6 | 40.0 | 35.0 | 1.6 | 1.44 |
| | 0.10 | | | | | 27.0 | 38.5 | 30.5 | 4.0 | 1.56 |

mixture of V–N and V–C and exhibit exceptional thermal stability at higher temperatures. The best mechanical properties may be ascribed to the formation of hard V–C bonds [9]. V–C–N thin films are produced by chemical and physical methods [9,14,17, and]. Therefore, the magnetron sputtering technique, allowing the production of fine thin films at low temperature (~300 °C) can be used for industrial deposition of films on various substrates. The elaboration of V–C–N thin films by reaction magnetron sputtering (in an argon–nitrogen atmosphere) was performed using V and C targets with different V/C atomic ratios under a nitrogen atmosphere [14] or with V target and addition of carbon and nitrogen containing reaction gases CH₄ and N₂ [15,17]. Another feature of the reactive magnetron sputtering technique is the possibility to produce ternary thin films, which offer interesting properties for industrial applications [18]. Mechanical and tribological properties of these hard films depend on the phases that compose the material. Vanadium carbonitride (V-C-N) is a ternary compound that combines the excellent chemical and wear resistance of V–N [18] and V–C [9], respectively. For these reasons, many researchers are interested in the ternary vanadium based compounds combining nitrides and carbides to improve film crystallization and its performance [19,20]. Their purpose was to establish the relationship between the microstructure and the mechanical properties of vanadium carbonitride. V-C-N coatings with different carbon contents were elaborated by Grigore et al. [21]. They observed that the film mechanical properties were improved with additional carbon and nitrogen content in V-C-N multilayers. The hardness of V-C-N films reached 3380 HV_{0.05}, being higher than that of binary VN (2970 HV_{0.05}) and VC (2770 HV_{0.05}) films, due to the formation of solid solution strengthening. However, limited reports are available about the effects of nitrogen on the structural, mechanical, and tribological properties of V-C-N [18–20].

Yu et al. [20] have studied the V-C-N films elaborated by magnetron sputtering using vanadium and carbon targets and a mixture of reactive Ar–N₂ gas. They investigated the influence of carbon content on the film structure. Excellent mechanical properties and wear resistance were obtained by adding carbon into the V–N matrix leading to form V-C-N solid solution. The influence of different (C + N)/V ratios on structure, mechanical properties and wear resistance of V-C-N coatings was comprehensively investigated. Previous reports on sputtered V-C-N coatings discussed either the microstructure and mechanical properties with different nitrogen content [18] or the influence of the V/(C + N) ratio on the mechanical and tribological behaviour without understanding the chemical bonding structure [20].

Thus, the purpose of the present study is to determine the influence of nitrogen partial pressure variation (P_{N₂}) during the sputtering process on the structure and composition of the V-C-N coatings and relate it to mechanical properties, adhesion and tribological performance of films.

2. Experimental methods

2.1. Deposition procedure

A series of V-C-N coatings was deposited using the radio frequency

(R.F, 13.56 MHz) magnetron sputtering technique (NORDIKO 3500), equipped with two V and C targets (99.99% purity, 106 mm in diameter). XC100 steel (with a chemical composition of (0.95 to 1.05) wt. % C, (0.5 to 0.8) wt.% Mn, 0.25 wt.% Si, 0.05 wt.% S, 0.035 wt.% (P and S), the balance being Fe) and Si (100) were used as substrates [5]. In order to enhance the quality of substrate surfaces to obtain an average roughness R_a of about 30 nm (determined by optical profilometry), samples were polished with Si–C carbide paper and diamond paste down to 1 μm. Then, these samples were cleaned in an ultrasonic bath with acetone and ethanol (5 min per sample) and dried in air.

The substrates were placed on the centre of the substrate-holder and its distance from the targets was fixed at 80 mm. The residual pressure was reduced to 2 × 10^{−5} Pa. Prior to deposition, the targets and substrates were cleaned by Ar⁺ ion bombardment for 5 min, applying a voltage of −700 V and −500 V, respectively.

The working pressure of 0.4 Pa was kept constant for all experiments. The coatings were deposited in a mixture of Ar (discharge gas) and N₂ (reactive gas) with different N₂/Ar ratios of 0/0.4, 0.02/0.38, 0.04/0.36, 0.06/0.34, 0.08/0.32, and 0.10/0.30 (Table 1). In order to keep a constant pressure, argon and nitrogen partial pressures were adjusted and their flow rates were controlled and regulated using MKS flow meters during the deposition process.

The V-C-N films with different nitrogen contents were deposited for 120 min with constant power (bias voltage) applied to V and C targets: 550 W (−900 V) and 150 W (−300 V), respectively. The deposition temperature was maintained at 150 °C and the sample holder rotation speed was set at 30 rpm in order to obtain uniform and homogeneous coatings. The deposition parameters and chemical composition of films are summarized in Table 1.

2.2. Characterizations: XRD, SEM, EDS, XPS, nanoindentation and tribotester

The crystallographic structure of the samples was investigated by X-ray diffraction (XRD) by means of a Siemens D5000 diffractometer. XRD analysis was carried out by using a CoK_α radiation line (λ = 1.78 Å) and applying 45 kV and 40 mA. The range of diffraction angles (2θ) was 25°–75° with a scanning speed of 2°/min. The average crystalline size of the coatings was determined with the Scherrer formula (Eq. (1)) [13]:

$$D = \frac{0.9 \lambda}{\beta \cdot \cos \theta} \quad (1)$$

where 0.9 is the shape factor, λ = 0.178 nm represents the X-ray wavelength of the radiation source, β is the peak width (full width half maximum, FWHM) in radians and θ is the Bragg's angle.

The morphology analysis of surfaces and cross-sections of the V-C-N coatings was carried out by using a Jeol JSM-6400F Scanning Electron Microscope (SEM). The chemical composition of the coatings was obtained by combining energy and wavelength dispersive X-ray spectroscopy (EDS, WDS).

The nature of the chemical bonds was investigated by X-ray photoelectron spectroscopy (Riber SIA 100 XPS, K_{αAl} = 1468.68 eV,

300 W). The vacuum in the spectrometer was 4×10^{-8} Pa. The spectrometer calibration was performed using binding energy level of C_{1s} (284.8 eV), which was absorbed on the surface of the samples. Then, the corresponding V_{2p} , C_{1s} and N_{1s} spectra were fitted under a multi-peak fitting method by using CasaXPS Software, and the ratio of Lorentzian to Gaussian was 20% [21].

The coating hardness and elastic modulus were determined by using a Nano Indenter XP, MTS Systems Corporation with continuous stiffness measurement (CSM) provided with a three-sided pyramidal diamond tip (Berkovich). Nanoindentation tests were carried out by applying a maximum load of 5 mN, 45 Hz of CSM frequency and 2 nm of oscillation amplitude. For each sample, 5 indentations were made, limiting the maximum indentation depth by up to 7% of the coating thickness in order to avoid the effect of substrate stiffness. The residual stresses were calculated from the sample-curvature radius using Stoney's formula (Eq. (2)) [22,23].

$$\sigma = \frac{E_s}{6(1-\nu_s)} \times \frac{t_s^2}{t_f} \left(\frac{1}{R} - \frac{1}{R_0} \right) \quad (2)$$

where the subscript S refers to the substrate, E_s (195 GPa) and ν_s (0.29) are the Young's modulus and Poisson ratio of Si (100) substrate, respectively. t_f and t_s are thicknesses of film and substrate, respectively. R_0 and R are the substrate curvature radii of the uncoated Si wafer and the coated Si wafer, which was determined by measuring the curvature of the silicon wafer before and after film deposition with a three-dimensional (3D) optical profilometer (VEECO, Wyko-NT 1100) [5].

The wear resistance of the coatings was investigated by using a TRIBO tester in dry conditions at room temperature. The ball-on-disc wear tests were performed by sliding against a 100Cr6 ball of 6 mm in diameter under a normal load of 2 N, at a constant sliding speed of $5 \text{ cm} \cdot \text{s}^{-1}$ and for a sliding distance of 200 m. The wear loss was quantified by measuring the profile of the wear track. The wear rates (W_R) of the films were calculated using the following equation (Eq. (3)) after calculating the wear track area with an optical profilometer:

$$W_R = \frac{\text{Wear volum}}{\text{Load} \times \text{Sliding distance}} \quad (3)$$

The substrate-film adhesion was evaluated by scratch tests using a Scratch Tester Millennium 200. Measurements were carried out using a conical diamond tip with a radius of 0.2 mm. The applied load was increased from 0.01 to 40 N with a constant loading speed of 0.01 mN/s. The stripping speed and length were 10 mm/min and 10 mm, respectively. The worn samples morphologies were observed by means of a SEM.

3. Results and discussion

3.1. Chemical composition

The influence of nitrogen partial pressure on the chemical composition of V-C-N films is presented in Fig. 1 and Table 1. We can see that increasing this pressure led to increase the N content gradually from 0 to 27 at.% and to decrease both V and C contents down to 38.50 at.% and 30.50 at.%, respectively. This result is in agreement with Schalk et al. [24] similarly showing a decrease in Al and Ti contents as a function of increasing nitrogen partial pressure. The partial pressures of nitrogen and argon were controlled and balanced in order to maintain the total pressure at a constant value by using MKS flowmeters during the films deposition. Increasing nitrogen partial pressure caused the poisoning of targets and the reduction of ionization leading consequently to a lower amount of vanadium and carbon during sputtering. This confirms the gradual decrease of the V and C deposition rates, with increasing nitrogen partial pressure. Consistently, by increasing the pressure of nitrogen from 0 to 0.10 Pa, the (N + C)/V ratio increased from 0.95 to 1.56. All films contained a small amount of oxygen

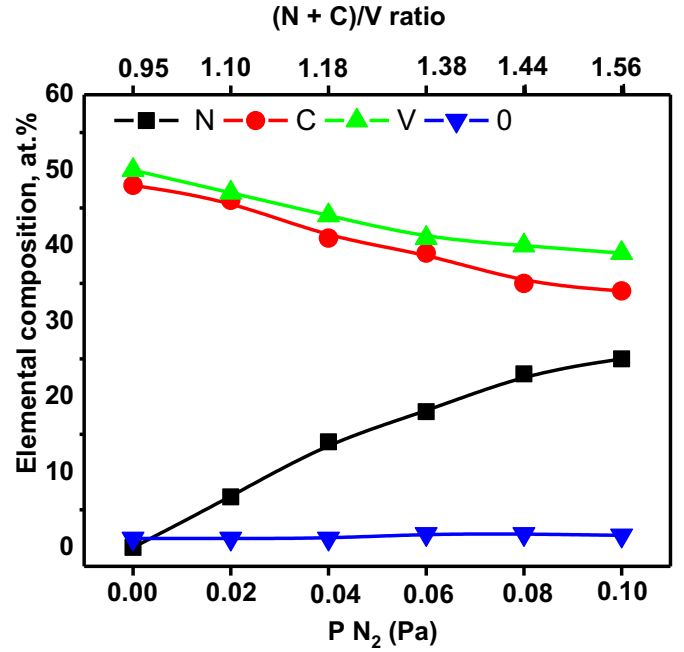


Fig. 1. Variation of chemical composition for V-C-N coatings as a function of nitrogen partial pressure.

(1.5–3 at.%), which might be induced by residual oxygen in the deposition chamber and contamination of the targets.

3.2. Microstructure

The evolution of the microstructure of V-C-N coatings with increasing P_{N_2} is shown in Fig. 2. At low diffraction angles (between 26° and 33°) small crystallographic planes emerge and indicate the presence of V_5O_9 phase (JCPDS card, No. 18-1450) for all coatings, which the oxygen mainly induced in the films and partly replaced the nitrogen and carbon. The diffraction patterns of films sputtered at 0 and 0.02 Pa show fcc-VC phase (JCPDS card, No. 07-0257) with strong diffraction from (111), (200) and (101) crystallographic planes at (43.9°), (47.4°) and (49.7°), respectively. The orthorhombic V_2C phase (JCPDS card, No. 71-1258) was also detected on (202) and (131) crystallographic

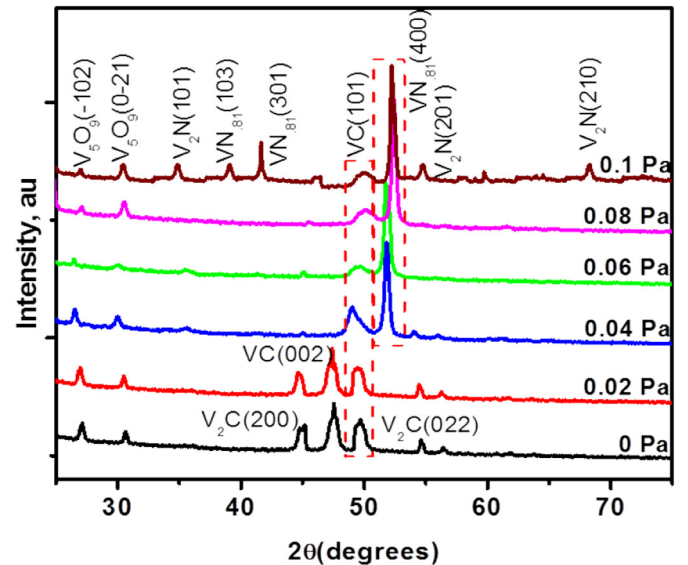


Fig. 2. X-ray diffraction patterns for V-C-N coatings sputtered at different nitrogen partial pressures.

planes corresponding to diffraction 2θ angles of 54.9° and 56° , respectively. The films sputtered with varying pressure between 0.04 and 0.08 Pa presented a significant reduction in V_2C and VC phases. The V_2C crystallographic plane is no longer visible and the intensity of (101) VC crystallographic plane becomes very low. The gradually weakened peaks indicate the poor crystallization of vanadium carbides. However, the XRD diffraction patterns show a high peak situated at 52.4° , representing a tetragonal (400) $VN_{.81}$ phase (JCPDS card, No. 71-1139). Also, the crystallographic planes at 54.78° assigning to the (201) reflection of V_2N was detected (JCPDS card, No. 71-0618). This is due to vanadium significantly exhibiting a more negative enthalpy when it combines with nitrogen.

The high quantity of nitrogen in film corresponding to a partial pressure of 0.10 Pa led to significantly change the film structure. From Fig. 2, we can see the appearance of several $VN_{0.81}$ crystallographic planes and the hexagonal V_2N phase related to the (101), (201) and (210) crystallographic planes located at 33.9° , 54.9° and 68.2° , respectively. It should be noted that all films deposited with different (N + C)/V ratios varied between 1.10 and 1.56 presented a dominant tetragonal $VN_{.81}$ phase similar to the tetragonal V_5N phase reported in reference [20].

Fig. 3 presents the variation of intensity, peak shift and FWHM as a function of nitrogen partial pressure for V-C-N coatings. These results were obtained for both (400) $VN_{.81}$ and (101) VC phases.

Generally, increasing pressure led to increase all these parameters for both phases except the intensity of (101) VC phase (Fig. 3). These changes in (101) VC and (400) $VN_{.81}$ peak intensities, FWHM and positions suggest that the distortion of the VC lattice occurs progressively as the nitrogen content in the coating increases. Addition of nitrogen led to a progressive replacement of the vanadium carbides by orthorhombic vanadium nitride resulting in a severe decrease in intensity accompanied by an increase in FWHM of the (101) VC. This is due to the poor crystallization of vanadium carbides and the moderate existence of carbon in the coatings in its amorphous state [25]. This is in good agreement with N. Schalk [24], who reported the decreasing of stress-free lattice parameters with increasing nitrogen content in the sputtered titanium aluminium nitride coatings. We can also relate these changes in coating microstructure to the compressive residual stress introduced in coatings, during sputtering, by the complex nature of the diffusion of vanadium, nitrogen and carbon atoms [23].

In order to determine the binding state, simultaneous XPS was carried out on the coatings. From Fig. 4, one can see that the coating surface mainly consists of V, C, and N. At 0.01 Pa, the high-resolution V2p spectrum shows peaks at the binding energies of the $V2p_{(3/2, 1/2)}$ (513.47 and 515.28 eV, FWHM 1.07 eV). The aforementioned peaks can be explained with three binding energies (Fig. 4a): peaks of $V2p_{3/2}$ (513.52 eV, FWHM 1.02 eV) and $V2p_{1/2}$ (515.13 eV, FWHM 2.22 eV) which are assigned to the V–C bond of the VC component [26,27], while the third peak of $V2p_{3/2}$ (513.12 eV, FWHM 1.16 eV) is assigned to V_2C [27]. Moreover, the C1s peak at the binding energy of

283.4 eV also demonstrates the presence of a C–V bond of VC (Fig. 4c) [27,28], which were supported by the XRD data. The results are similar to those reported in the literature for VC phase [29]. For the N1s XPS spectra (397.44 eV, FWHM 1.56 eV) (Fig. 4e), the main peak of N1s corresponds to V_2N (397.40 eV, FWHM 1.54 eV) [5] and the minor peak corresponds to VN_x (297.80 eV, FWHM 2.82 eV) [30]. These results mean that vanadium carbide and nitride coexist in the coating as shown from the XRD analysis (Fig. 2).

At 0.06 Pa, we notice a significant decrease in the C1s spectra intensity and changes in the V and N1s spectra. A positive shift from 513.47 up to 514.21 eV for the peaks of V2p is observed. The $V2p_{(3/2, 1/2)}$ (514.21 and 521.61 eV, FWHM 2.25 eV) spectra can be fitted into four peaks, located at about (513.81 eV, FWHM 1.39 eV), (516.7 eV, FWHM 2.89 eV) (517.31 eV, FWHM 2.36 eV) and (522.079 eV, FWHM 2.46 eV) (Fig. 4b), corresponding to $VN_{.81}$, V_2N , VC and VO_x [5,31]. The C1s spectrum is located at a binding energy of 282.86 eV (Fig. 4d). Through Gaussian fitting analysis, the peaks at (282.84 eV, FWHM 1.20 eV) and (283.67 eV, FWHM 3.07 eV) correspond to V–C and C–N bonds [26,32]. This indicates that the C–N binding is weakly formed in the V-C-N coatings after incorporation of nitrogen atoms and confirms the coexistence of vanadium nitride and carbide phases in the V-C-N system at high nitrogen content. However, the vanadium carbonitrides do not appear in the XRD diffraction patterns (Fig. 2), showing that the content of vanadium carbonitride is very low. The peak size of N1s between 397.36 and 398.78 eV becomes large and asymmetric (Fig. 4f). The main peak of N1s spectra corresponds to $VN_{.81}$ (397.25, FWHM 2.42 eV) and the minor peak corresponds to V_2N (398.56 eV, FWHM 2.42 eV) [5,30]. However, the third peak corresponds to N–C bond (398.39 eV, FWHM 1.60 eV) [32]. The XRD and XPS analysis results reveal that V-C-N coatings are an interstitial (V–C, V–N) mixture, which exhibits a crystalline structure. However, the V–C binding intensity decreases gradually while V–N binding increases. This suggests that V–N and V–C bonds coexist in the coatings and the content of $VN_{.81}$ increases while the VC content decreases with increasing N content.

3.3. Morphology

SEM images showing the cross section and surface morphology of V-C-N coatings are represented in Fig. 5. Fig. 6 presents the variation of film thickness, growth rate and crystallite size of films deposited at different nitrogen partial pressures. One can notice that the surface of coatings sputtered at low pressure varied between 0 and 0.04 Pa, revealing a porous surface with fine grains of 14 and 12 nm respectively (Fig. 5). The films deposited at $P_{N_2} = 0.06$ Pa present uniform and fine grains. Increasing the pressure led to decrease the growth rate of V-C-N films (Fig. 6). In fact, the addition of nitrogen led to modify the growth mode of films with the presence of amorphous carbon. By increasing the pressure up to 0.08 Pa, significant changes in coating morphology were observed such as pyramidal like sharp grains (26 nm in size, Figs. 5 and

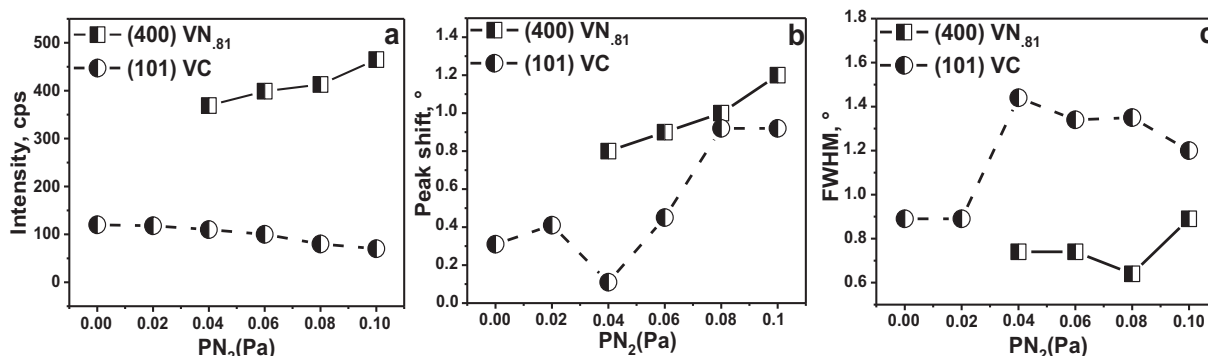


Fig. 3. Intensity (a), peak shift (b) and FWHM (c) versus nitrogen partial pressure for V-C-N coatings presenting (400) $VN_{.81}$ and (101) VC peaks.

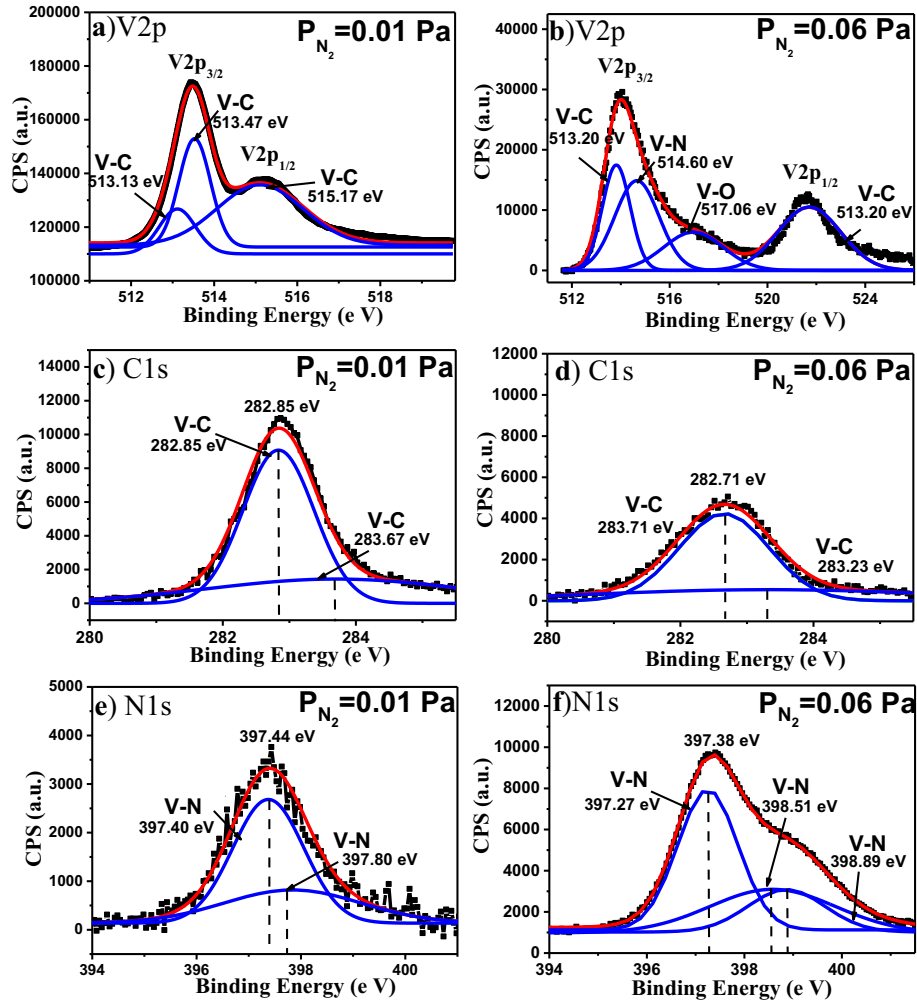


Fig. 4. The fitted (a, b) V2p, (c, d) C1s and (e, f) N1s XPS spectra for V-C-N coatings deposited at $P_{N_2} = 0.01$ and 0.06 Pa.

6). The pyramidal grain size increased gradually with increasing pressure from 0.08 to 0.10 Pa (Figs. 5 and 6). In our previous study [29], we reported a similar evolution of the morphology of V-N coatings deposited by the same procedure, which is a result of the mutual interference of the intermediate VN and V_2N phases.

The grain size of V-C-N films sputtered at $P_{N_2} > 0.06$ Pa clearly increased simultaneously with decreasing the film thickness. The grain coalescence, performed with increasing the N content in films, is due to the reduction of ion bombardment energy during the reactive sputtering of V, C and N elements and the re-nucleate on the V-N compounds through film deposition [3].

Cross-sectional SEM images (Fig. 5) show a columnar morphology for all coatings with different column widths. A similar morphology was reported by Bondarev et al. [18].

We noticed that a superficial thin oxide layer was subsequently formed, the thickness of which depends on the applied nitrogen partial pressure. Its maximum value ($\approx 0.11 \mu\text{m}$) was measured for the film deposited at 0.04 Pa, which contained about 3.4 at.% of oxygen. The formation of this oxide layer is due to the reduction in dense structure caused by the low kinetic energy of incidence ions, which increased nucleation of oxides during film growth [33]. From Fig. 6, we can clearly see that growth rate and film thickness, evaluated by SEM, decrease from $0.0022 \mu\text{m}/\text{min}$, $2.41 \mu\text{m}$ (at 0 Pa) to $0.0013 \mu\text{m}/\text{min}$, $1.60 \mu\text{m}$ (at 0.10 Pa), respectively. This behaviour can also be explained by the pollution of the target and the re-nucleation of the vanadium nitrides through film deposition. It may also be slightly affected by the low compact solid solution, which decreases by increasing nitrogen

content as compared to the V-C coatings [34,35].

3.4. Mechanical properties

To investigate the mechanical behaviour of the V-C-N films sputtered at different nitrogen partial pressures, nanoindentation measurements were performed. Fig. 7(a) illustrates the typical load-displacement curves obtained from these tests. It can be shown that these curves are superimposed at low loads < 100 mN, signifying that elastic deformation is dominant at this stage for all coatings [29].

The maximum applied load was about 700 mN, which allowed achieving maximum indentation depths (Fig. 7a, b). With a limit of 7% of total film thickness, it clearly shows a stiffer plastic response, as is demonstrated by the lower indentation depth and greater loading curvature.

This response results in a smaller depth with an equivalent maximum load than compared with load-displacement curves without taking a limit of 10% of total film thickness. Suggesting the V-C-N films are more resistant to plastic deformation than a steel substrate; this qualitative analysis confirmed the inactive effect of the substrate on the hardness values (Fig. 7a, b). It can also easily be seen that the load-displacement curves stabilized as the film thickness increased, which can be explained by strain gradient effect or the Hall-Petch effect [36]. Also, the higher the nitrogen pressure, the higher the penetration depth is. This indicates that the plastic deformation of vanadium nitrides is lower than that of vanadium carbides.

Mechanical properties of coatings sputtered at different P_{N_2} are

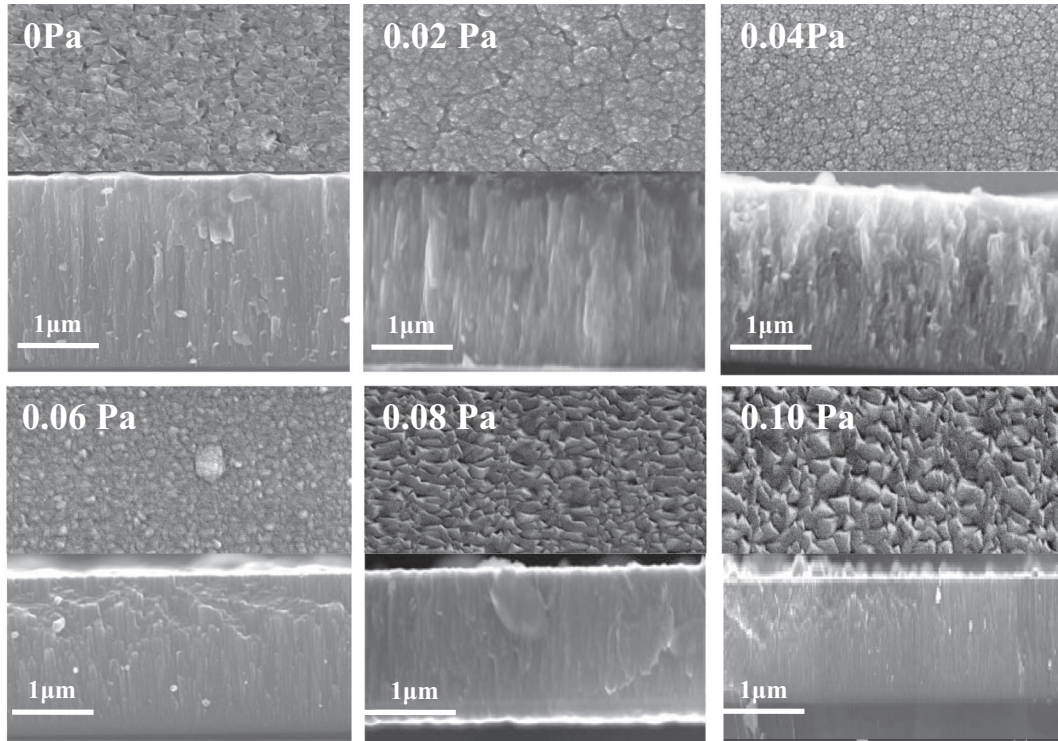


Fig. 5. SEM images of surface and cross-sections for V-C-N coatings sputtered at different nitrogen partial pressures.

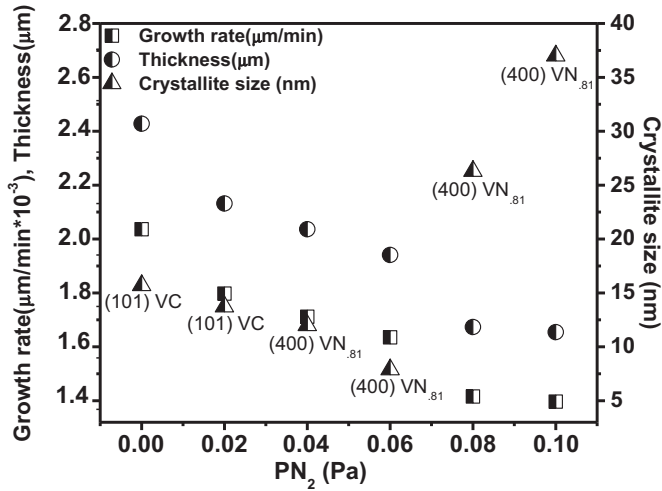


Fig. 6. Growth rate, film thickness and crystallite size for V-C-N coatings sputtered at different nitrogen partial pressures.

summarized in Fig. 7(c) and Table 2. The coating hardness (H) and elastic modulus (E) increased with an increase of P_{N_2} up to 0.06 Pa and then, beyond this value, they decreased gradually. The H and E values were measured with considering 7% of total film thickness. For a pure VC coating, the average hardness value was 15 GPa. We find that the V-C-N films have a significant increase in hardness and elastic modulus, from ($H = 17 \pm 2$ GPa, $E = 220 \pm 10$ GPa) at $P_{N_2} = 0.02$ Pa to ($H = 26.1 \pm 1.0$ GPa, $E = 268 \pm 10$ GPa) at $P_{N_2} = 0.06$ Pa (Fig. 7c). This can be explained by the increasing density and sub-stoichiometric films with a mixture of vanadium carbide and nitride phases. According to XPS analysis, the peak shift of V2p binding energy suggests that the bonding character changed from V-C to harder V-N bonds due to the N insertion through V atoms [23,37].

From Fig. 2, the XRD diffraction pattern of the film sputtered at 0.06 Pa shows a major (400) VN_{.81} peak indicating the effect of solid

solution strengthening of the V-C-N coating by nitrogen atoms incorporation and grain refinement [2,32]. At a higher P_{N_2} , the structure was polycrystalline and the (N + C)/V ratio further increased and reached 1.56 at $P_{N_2} = 0.10$ Pa. This is considerably higher than that of VN_{.81} and VC phases, typically exhibiting a decrease in the hardness and elastic modulus, which is consistent with several works in the literature [19,38]. It seems that the low hardness of coatings deposited at $P_{N_2} = 0.10$ Pa is due to the large grain size (37 nm, Fig. 5) and the low film thickness according to the Hall-Petch relation [19]. Furthermore, the V-C-N coating suffers from significant oxygen contamination which typically reacts with vanadium, forming oxides and affects harmfully the mechanical properties [5].

The elastoplastic behaviour of coatings can be investigated by H/E and H^3/E^2 ratios. Both ratios are related to the toughness of the coatings [31] varied similarly. The highest elastic and plastic strain ratios of 0.097 and 0.224 GPa respectively, were obtained for the coating deposited at 0.06 Pa. This is mostly a consequence of the low elastic modulus value, as compared to those of other hard films [25–33]. The addition of nitrogen led to significantly change the chemical composition, in particular the (N + C)/V ratio (Fig. 1), and consequently the microstructure of the coatings (Figs. 2 and 5). The H/E and H^3/E^2 ratios of all V-C-N films, except the film deposited at 0.1 Pa, are higher than that of a pure VC coating [20].

The values of residual stresses calculated from the sample-curvature radius using Stoney's formula are shown in Table 2. We found that compressive residual stresses produced during sputtering in pure VC were -2.2 GPa. By increasing the nitrogen pressure, the lowest value of this stress was measured in the film sputtered at 0.06 Pa (0.4 GPa). The drop in residual stress with the addition of nitrogen can be explained by the changes in film growth due to the incorporation of nitrogen in the vanadium lattice. We found that mechanical properties of V-C-N coatings deposited at 0.06 Pa were close to those previously reported for V-C-N coatings with N + V = 83.01 at.%, and C = 16.89 at.% [20]. Moreover, the drop in the mechanical properties can be explained by the relaxation of residual stress and the formation of V₂N phase at high nitrogen content, which is less dense as compared to the VN_{.81} phase

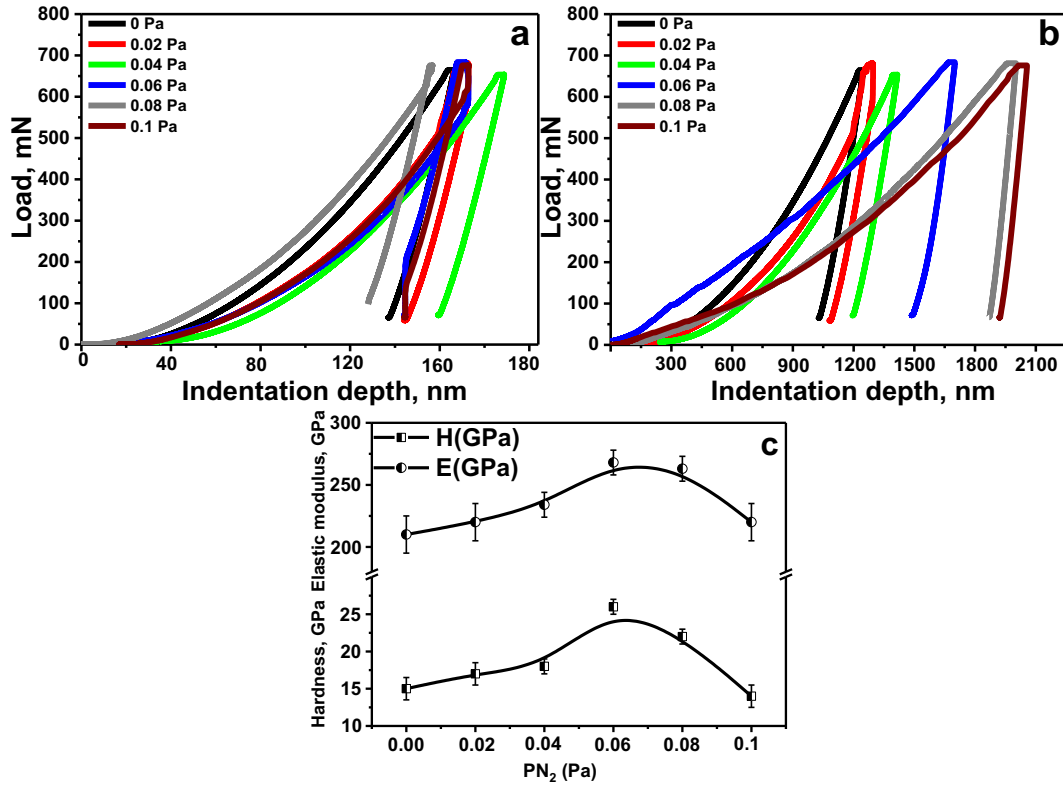


Fig. 7. Load-displacement curves as a function of the indenter penetration depth: a) maximum penetration limited to 7% of the total film thickness, b) without limited penetration and c) hardness and elastic modulus for V-C-N coatings sputtered at different nitrogen partial pressures.

Table 2
Mechanical properties of V-C-N coatings.

| PN ₂ , Pa | 7% of total film thickness, nm | H, GPa | E, GPa | H/E | H ³ /E ² , GPa | R. stresses, (GPa) |
|----------------------|--------------------------------|--------|----------|-------|--------------------------------------|--------------------|
| 0 | 168 | 15 ± 2 | 210 ± 10 | 0.071 | 0.077 | 2.2 |
| 0.02 | 147 | 17 ± 2 | 220 ± 10 | 0.077 | 0.102 | 1.9 |
| 0.04 | 140 | 18 ± 1 | 234 ± 10 | 0.077 | 0.107 | 1.6 |
| 0.06 | 133 | 26 ± 1 | 268 ± 10 | 0.097 | 0.245 | 0.4 |
| 0.08 | 114 | 22 ± 1 | 263 ± 10 | 0.083 | 0.154 | 0.5 |
| 0.1 | 112 | 14 ± 2 | 220 ± 10 | 0.063 | 0.057 | 0.8 |

[5].

3.5. Tribological properties

3.5.1. Friction

Fig. 8 shows the friction coefficient curves of the V-C-N coatings sputtered at different nitrogen partial pressures. The friction coefficients of all V-C-N coatings are characterized by two different parts. For V-C-N, the friction coefficient (CoF) is not constant during the test. An initial running-in period, during which the CoF rises rapidly can be observed, which represents a transition pattern of friction for rough surfaces. This is followed by a steady-state region which varies from test to test, from a minimum of 3 m of the total sliding distance [39].

Surface roughness (RMS) and friction coefficient (CoF) of V-C-N coatings deposited at different nitrogen pressures are presented in Table 3. The RMS value of VC film was close to that of a V-C-N coating deposited at 0.02 Pa. From Table 3, we can note that increasing the nitrogen pressure led to significantly decrease the coating roughness, which may be due to the competitive growth between vanadium carbides and nitrides [23]. The low surface roughness can affect friction and wear performance during the sliding test. The CoF average of the V-C-N coating, measured against a 100Cr6 ball, was 0.42 at 0.06 Pa

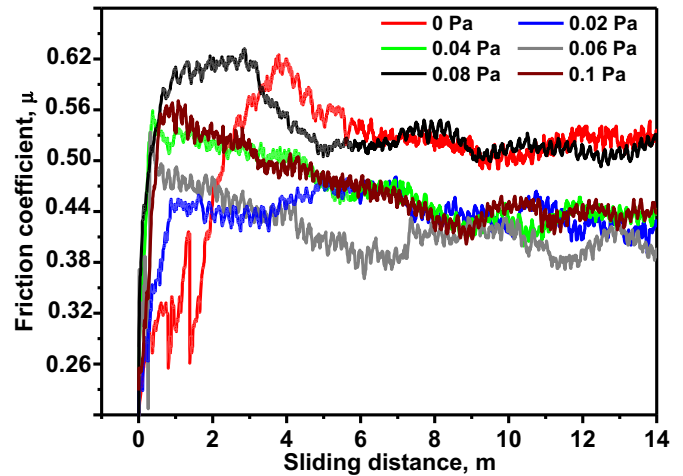


Fig. 8. Friction coefficient vs. the sliding distance for the V-C-N coatings sputtered at different nitrogen partial pressures.

Table 3
Roughness and tribological properties of V-C-N coatings.

| PN ₂ , Pa | Roughness | Tribological properties | |
|----------------------|-----------|-------------------------|---|
| | RMS, nm | CoF | W _R (× 10 ⁻⁷), mm ³ /Nm |
| 0 | 41 | 0.62 | 11.30 |
| 0.02 | 37 | 0.58 | 8.21 |
| 0.04 | 26 | 0.56 | 4.25 |
| 0.06 | 8 | 0.44 | 2.22 |
| 0.08 | 10 | 0.47 | 2.66 |
| 0.10 | 11 | 0.56 | 4.20 |

(Fig. 8) close to the values reported by Ge et al. [40].

The CoF values for the V-C-N coatings deposited at different P_{N_2} varying from 0.04 to 0.08 Pa were similar to those previously reported by Bondarev and Yu [18,20] indicating a positive influence of nitrogen addition. The V-C-N coating deposited at 0.10 Pa unexpectedly demonstrated a high CoF value which can be explained by the decrease in the VN_{81} phase with a significant $(N + C)/V$ ratio = 1.65. In fact, nitrogen addition causes surface softness of V-C-N films ($H = 14$ GPa) leading to increase the contact area and consequently the friction force during sliding test [39]. Thus, these results are in partial accordance with a previous study showing a decrease in the CoF [18]. According to our previous study [8], the decrease in the CoF is also attributed to the contamination of the V-C-N coating by oxygen and the formation of vanadium oxides. These oxides act as a lubricant between the film surface and the ball resulting in a low friction coefficient. The decrease in the surface roughness of V-C-N coatings having a higher $(N + C)/V$ ratio indicates the negative influence of a low carbon content in the coatings [18].

3.5.2. Wear

Micrographs and cross-sectional wear track depth profiles of the V-C-N samples are presented in Fig. 9. The wear rate values are presented in Table 3. For the films deposited at a low nitrogen pressure ≤ 0.04 Pa, the spallation failure mode is observed and the total delamination of the V-C-N films is due to the low resistance to plastic deformation (Fig. 7a) [23]. The V-C-N coatings deposited at 0.06 and 0.08 Pa confirm an especially good wear resistance; their wear rates are in the range of $2.66 \times 10^{-7} \text{ mm}^3/\text{Nm}$. A little abrasion wear is observed in the middle of wear tracks parallel to the sliding direction, which is attributed to its low surface roughness and high hardness value [18,23]. The SEM images of coatings sputtered at 0.04 and 0.10 Pa show a significant amount of wear debris accumulated on the wear track and the wear rate for both films is $4.20 \times 10^{-7} \text{ mm}^3/\text{Nm}$. This result indicates that abrasion is due to the low resistance of films to plastic strain, which is

expected in ductile films [18,41].

3.5.3. Adhesion

Scratch tests were carried out on V-C-N coatings by applying different loads of 5, 20 and 40 N. The scratch tracks were investigated to evaluate the influence of nitrogen partial pressure on the film adhesion and to reveal the damage nature between the coating and the XC100 substrate. The SEM images of scratch tracks are presented in Fig. 10. For all samples; applying a low charge of 5 N did not cause any failure in the scratch track. A further increase in the applied load to 10 N led to initiate and propagate cracks through coatings. Wear track morphology of V-C-N deposited at 0.06 Pa was relatively smooth. We did not observe spallation or delamination of the coating. However, some chipping of layers at the edges of the scratch can be observed. The wear tracks of V-C-N coatings sputtered at 0 and 0.10 Pa have a very rough surface. The track becomes broader and the conformal cracks along the scratch edge are visible. This is a typical brittle-ductile behaviour in V-C-N coatings [29]. The cohesive failure of the V-C-N coatings is a response to the internal stress developed within the coatings during the test where cracking occurs in high stress areas [22,42].

By increasing the applied load up to 40 N, it can be seen that the wear resistance of the very hard V-C-N coatings is even higher than that of the V-C coating. This adhesive feature is confirmed by the characteristics of the wear track. For the V-C-N coating deposited at 0.06 Pa, the wear track reveals few cracks. According to Sun et al. [42], the transition-metal carbonitride coatings become harder when the energy of crack propagation decreases with the reduction of the carbon content, which is in agreement with our results. However, all coatings present deterioration, an obvious delamination and cracks on track edges of the scratch. The plastic deformation along the tracks is caused by tensile stress behind the sliding stylus [43].

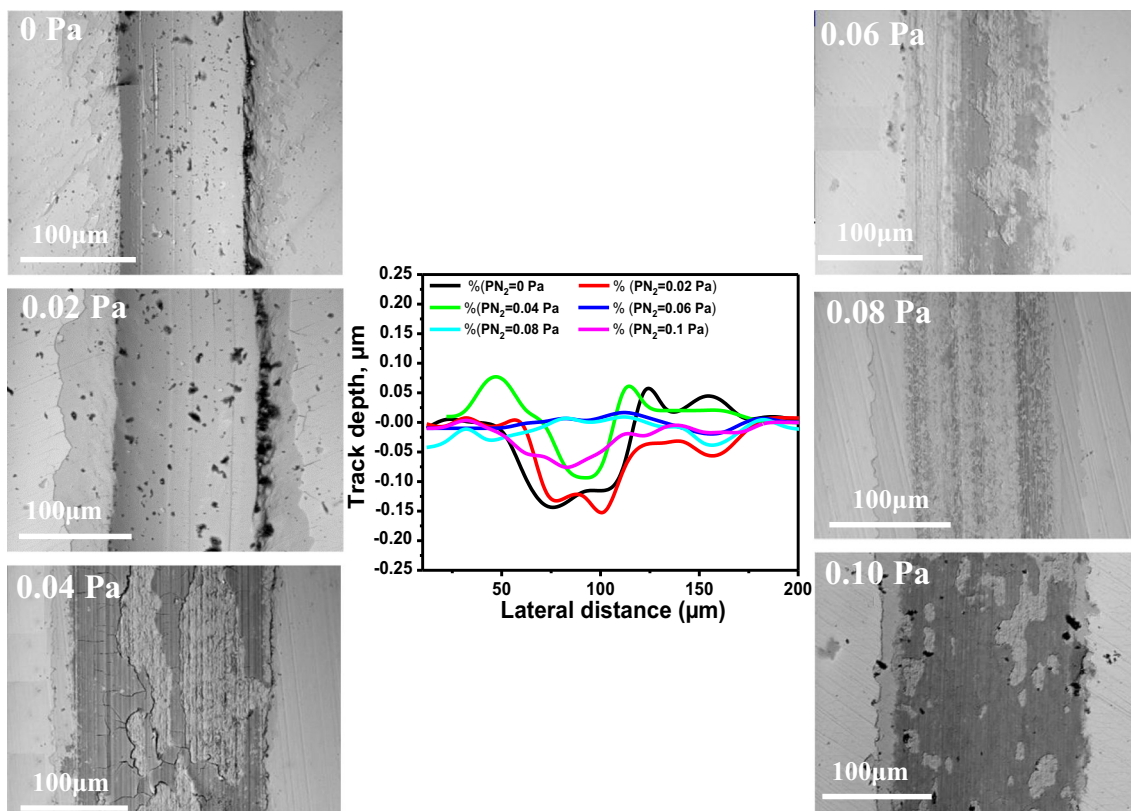


Fig. 9. SEM wears track images and track depth for V-C-N coatings sputtered at different nitrogen partial pressures.

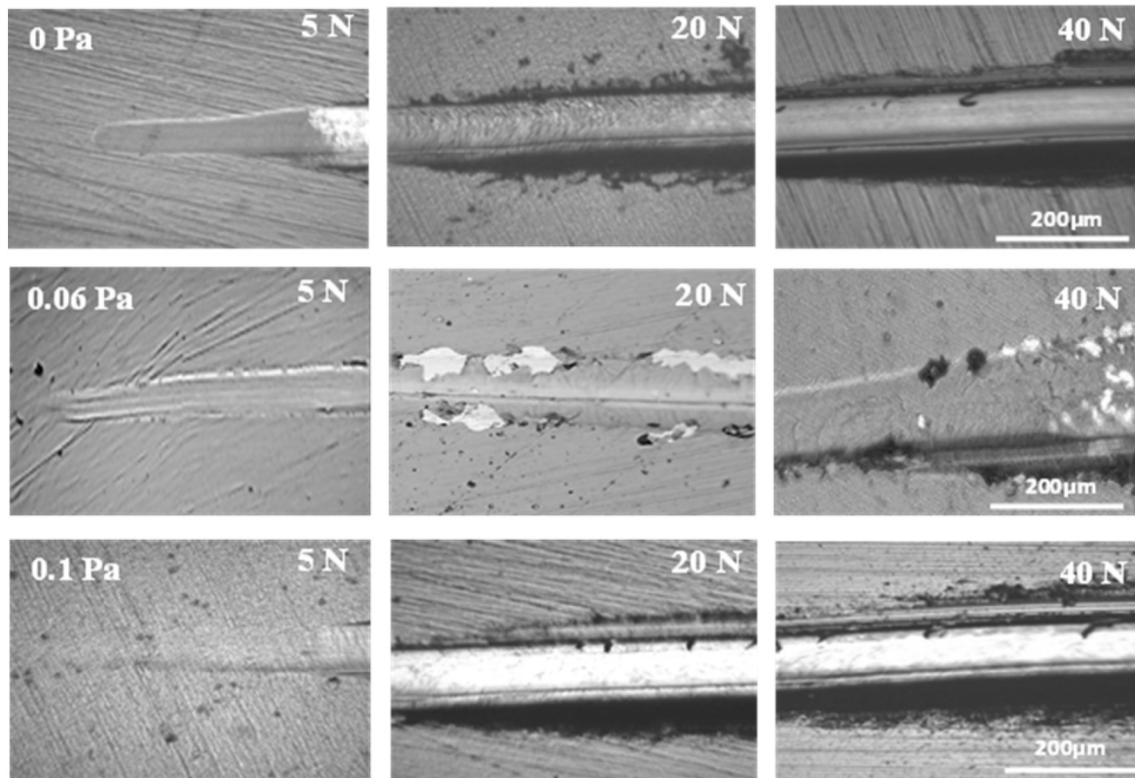


Fig. 10. SEM images for V-C-N coatings, deposited on XC100 substrates, after scratch track tests.

4. Conclusion

In this paper, the effects of nitrogen partial pressure on the structure, morphology, mechanical and tribological properties of the Vanadium carbonitride magnetron sputtered coatings were investigated.

- ✓ V-C-N coatings sputtered at low pressure ≤ 0.04 Pa consisted of solid solution of fcc-VC and hcp-V₂C. Increasing the nitrogen partial pressure led to change the microstructure of the films to hcp-V₂N and t-VN₈₁ phases. This is due to the incorporation of nitrogen through the vanadium lattice. However, the VC carbide appeared in low amounts at 0.10 Pa.
- ✓ It was demonstrated that the porous morphology changes to a dense one with a pyramid like peak when nitrogen atoms are incorporated into the vanadium lattice.
- ✓ The hardest V-C-N film was sputtered at 0.06 Pa of nitrogen partial pressure with the formation of a vanadium carbide and nitride mixture. Its value of 26.1 GPa was obtained with $(N + C)/V = 1.44$. This film showed an excellent strength to elastoplastic deformation. The mechanical parameters of V-C-N films gradually decreased with grain coalescence.
- ✓ The V-C-N film sputtered at 0.06 Pa revealed the lowest friction coefficient (0.42) and the best wear performance. However, increasing the nitrogen partial pressure to > 0.08 Pa led to a decrease in the film resistance to plastic strain and the total delamination of all the V-C-N coatings.

Acknowledgements

The authors would like to thank the support of PVD Coatings Project for the equipment supplied by the La.Bo.Ma.P at Arts et Metiers ParisTech of Cluny, which was used in this study. We would like to thank Pr. IMHOFF for the XPS and SEM analysis of the test samples.

References

- [1] M.T. Hosseinejad, M. Ghorannevis, G.R. Etaati, M. Shirazi, Z. Ghorannevis, Deposition of tungsten nitride thin films by plasma focus device at different axial and angular positions, *Appl. Surf. Sci.* 257 (2011) 7653–7658.
- [2] H. Zhao, Z. Ni, F. Ye, Structure and mechanical properties of reactive sputtered WCN films, *Surf. Eng.* 32 (4) (2016) 307–313.
- [3] C.P. West, I. Harrison, E.J. Cussen, D.H. Gregory, Facile synthesis of bimetallic carbonitrides, V_{1-x}Ti_x(C, N), by microwave carbothermal reduction-ammonolysis/carburisation (MW-CRAC) methods, *J. Eur. Ceram. Soc.* 29 (2009) 2355–2361.
- [4] N.S. Gajbhiye, R.S. Ningthoujam, Low temperature synthesis, crystal structure and thermal stability studies of nanocrystalline VN particles, *Mater. Res. Bull.* 41 (2006) 1612–1621.
- [5] L. Aissani, C. Nouveau, M.J. Walock, H. Djebaili, A. Djelloul, Influence of vanadium on structure, mechanical and tribological properties of CrN coatings, *Surf. Eng.* 31 (10) (2015) 779–788.
- [6] Y. Qiu, S. Zhang, B. Li, J.-W. Lee, D. Zhao, Influence of nitrogen partial pressure and substrate bias on the mechanical properties of VN coatings, *Procedia Eng.* 36 (2012) 217–225.
- [7] K. Sarakinos, J. Alami, D. Severin, P.M. Karimi, M. Wutti, The effect of the back-scattered energetic atoms on the stress generation and the surface morphology of reactively sputtered vanadium nitride films, *Thin Solid Films* 516 (14) (2008) 4568–4573.
- [8] C. Aguzzoli, C.A. Figueroa, F.S. Souza, A. Spinelli, I.J.R. Baumvol, Corrosion and nanomechanical properties of vanadium carbide thin film coatings of tool steel, *Surf. Coat. Technol.* 206 (2012) 2725–2731.
- [9] C.K.N. Oliveira, C.L. Benassi, L.C. Casteletti, Evaluation of hard coatings obtained on AISID2 steel by thermo-reactive deposition treatment, *Surf. Coat. Technol.* 201 (2006) 1880–1885.
- [10] L. Wu, T. Yao, Y. Wang, J. Zhang, F. Xiao, B. Liao, Understanding the mechanical properties of vanadium carbides: nano-indentation measurement and first-principles calculations, *J. Alloys Compd.* 548 (2013) 60–64.
- [11] R. Teghil, A.D. Bonis, A. Galasso, P. Villani, A. Santagata, D. Ferro, S.M. Barinov, Nanostructured thin films obtained by ultra-short pulse laser deposition of vanadium carbide, *Appl. Surf. Sci.* 255 (2009) 5220–5223.
- [12] X. Zhang, B. Wang, Z. Zhan, F. Huang, Microstructure, chemical states, and mechanical properties of V-C-Co coatings prepared by non-reactive magnetron sputtering, *Thin Solid Films* 540 (2013) 135–141.
- [13] E. Portolan, C.L.G. Amorim, G.V. Soares, C. Aguzzoli, C.A. Perottoni, I.J.R. Baumvol, C.A. Figueroa, Carbon occupancy of interstitial sites in vanadium carbide films deposited by direct current reactive magnetron sputtering, *Thin Solid Films* 517 (24) (2009) 6493–6496.
- [14] U. Jansson, E. Lewin, Sputter deposition of transition-metal carbide films — a critical review from a chemical perspective, *Thin Solid Films* 536 (2013) 1–24.
- [15] M.E. Launey, R.O. Ritchie, On the fracture toughness of advanced materials, *Adv.*

- Mater. 21 (2009) 2103–2110.
- [16] O.Y. Khyzhun, V.A. Kolyagin, Electronic structure of cubic and rhombo-hedral tantalum carbonitrides studied by XPS, XES, and XAS methods, *J. Electron. Spectrosc. Relat. Phenom.* 137–140 (2004) 463–467.
- [17] C. Mitterer, N. Fateh, F. Munnik, Microstructure–property relations of reactively magnetron sputtered VC_xN_y films, *Surf. Coat. Technol.* 205 (13–14) (2011) 3805–3809.
- [18] A.V. Bondarev, M. Golizadeh, N.V. Shvyndina, I.V. Shchetinin, D.V. Shtansky, Microstructure, mechanical, and tribological properties of Ag-free and Ag doped VCN coatings, *Surf. Coat. Technol.* 331 (2017) 77–84.
- [19] C.L. Yeh, Y.D. Chen, Combustion synthesis of vanadium carbonitride from V-C powder compacts under nitrogen pressure, *Ceram. Int.* 33 (2007) 365–371.
- [20] L. Yu, Y. Li, H. Ju, J. Xu, Microstructure, mechanical and tribological properties of magnetron sputtered VCN films, *Surf. Eng.* 33 (2017) 919–924.
- [21] E. Grigore, C. Ruset, C. Luculescu, The structure and properties of VN-VCN-VC coatings deposited by a high energy ion assisted magnetron sputtering method, *Surf. Coat. Technol.* 205 (2) (2011) S29–S32.
- [22] E. Grigore, C. Ruset, X. Li, H. Dong, The influence of carbon content on the characteristics of V–C–N coatings deposited by combined magnetron sputtering and ion implantation (CMSII), *Surf. Coat. Technol.* 204 (2010) 2006–2009.
- [23] L. Aissani, M. Fellah, C. Nouveau, M.A. Samad, A. Montagne, A. Iost, Structural and mechanical properties of Cr–Zr–N coatings with different Zr content, *Surf. Eng.* 34 (2017) 1–9.
- [24] N. Schalk, J. Simonet Fotso, D. Holec, G. Jakopic, A. Fian, V. Terziyska, R. Daniel, C. Mitterer, Influence of varying nitrogen partial pressures on microstructure, mechanical and optical properties of sputtered TiAlON coatings, *Acta Mater.* 119 (2016) 26–34.
- [25] X. Wu, G. Li, Y. Chen, G. Li, Microstructure and mechanical properties of vanadium carbide coatings synthesized by reactive magnetron sputtering, *Int. J. Refract. Met. Hard Mater.* 27 (2009) 611–614.
- [26] F. Liu, Y. Yao, H. Zhang, Y. Kang, G. Yin, Z. Huang, X. Liao, X. Liang, Synthesis and characterization of vanadium carbide nanoparticles by thermal refluxing-derived precursors, *J. Mater. Sci.* 46 (2011) 3693–3697.
- [27] G. Greczynski, D. Primetzhofer, L. Hultman, Reference binding energies of transition metal carbides by core-level X-ray photoelectron spectroscopy free from Ar⁺ etching artefacts, *Appl. Surf. Sci.* 436 (2018) 102–110.
- [28] R. Teghil, A. De Bonis, A. Galasso, P. Villani, A. Santagata, D. Ferro, S.M. Barinov, Nanostructured thin films obtained by ultra-short pulse laser deposition of vanadium carbide, *Appl. Surf. Sci.* 255 (2009) 5220–5223.
- [29] X. Cai, L. Zhong, Y. Xu, Z. Lu, J. Li, J. Zhu, Y. Ding, H. Yan, Microstructural characterization of a V₂C and V₈C₇ ceramic-reinforced Fe substrate surface compound layer by EBSD and TEM, *J. Alloys Compd.* 747 (2018) 8–20.
- [30] J.H. Ouyang, S. Sasaki, The friction and wear characteristics of cathodic arc ion-plated (V, Ti) N coatings in sliding against alumina ball, *Wear* 257 (7–8) (2004) 708–720.
- [31] J.-G. Choi, The surface properties of vanadium compounds by X-ray photoelectron spectroscopy, *Appl. Surf. Sci.* 148 (1999) 64–72.
- [32] L. Aissani, M. Fellah, L. Radjeji, C. Nouveau, A. Montagne, A. Alhussein, Effect of annealing treatment on the microstructure, mechanical and tribological properties of chromium carbonitride coatings, *Surf. Coat. Technol.* 359 (2019) 403–413.
- [33] L. Aissani, C. Nouveau, M.J. Walock, H. Djebaili, A. Djelloul, Influence of vanadium on structure, mechanical and tribological properties of CrN coatings, *Surf. Eng.* 31 (10) (2015) 779–788.
- [34] C.I. Enriquez-Flores, E. Cruz-Valeriano, A. Gutierrez-Peralta, J.J. Gervacio-Arciniega, E. Ramírez-Álvarez, E. Leon-Sarabia, J. Moreno-Palmerin, Relation between work function, microstructural and mechanical properties of TiN-films, *Surf. Eng.* 34 (2018) 660–666.
- [35] P. Stoyanov, J. Schneider, M. Rinke, S. Ulrich, E. Nold, M. Dienwiebel, M. Stüber, Microstructure, mechanical properties and friction behavior of magnetron-sputtered V-C coatings, *Surf. Coat. Technol.* 321 (2017) 366–377.
- [36] S. Chen, L. Liu, T. Wang, Investigation of the mechanical properties of thin films by nanoindentation, considering the effects of thickness and different coating–substrate combinations, *Surf. Coat. Technol.* 191 (2005) 25–32.
- [37] C. Ramoul, N.E. Beliardouh, R. Bahi, C. Nouveau, A. Djahoudi, M.J. Walock, Surface performances of PVD ZrN coatings in biological environments, *Tribol. Mater. Surf. Interfaces* 13 (1) (2019) 12–19.
- [38] C. Aguzzoli, C.A. Figueroa, F.S. de Souza, A. Spinelli, I.J.R. Baumvol, Corrosion and nanomechanical properties of vanadium carbide thin film coatings of tool steel, *Surf. Coat. Technol.* 206 (2012) 2725–2731.
- [39] G. Cassar, J.C. Avelar-Batista Wilson, S. Banfield, J. Housden, A. Matthews, A. Leyland, A study of the reciprocating-sliding wear performance of plasma surface treated titanium alloy, *Wear* 269 (2010) 60–70.
- [40] F. Ge, X. Zhou, F. Meng, Q. Xue, F. Huang, Tribological behavior of VC/Ni multilayer coatings prepared by non-reactive magnetron sputtering, *Tribol. Int.* 99 (2016) 140–150.
- [41] L. Milschi, I. Belahsen, G.C. Lain, S.S. Tomiello, C.D. Boeira, L.T. Bim, F. Cemin, C.M. Menezes, B.L. Perotti, J. Catafesta, C.A. Figueroa, Optical and tribological properties of decorative titanium carbonitride coatings, *Surf. Eng.* 34 (2018) 562–568.
- [42] Y. Sun, C. Lu, H. Yu, A.K. Tieu, L. Su, Y. Zhao, H. Zhu, C. Kong, Nanomechanical properties of TiCN and TiCN/Ti coatings on Ti prepared by filtered arc depositions, *Mater. Sci. Eng. A* 625 (2015) 56–64.
- [43] C. Sun, Q. Xue, J. Zhang, S. Wan, A.K. Tieu, B.H. Tran, Growth behavior and mechanical properties of Cr-V composite surface layer on AISI D3 steel by thermal reactive deposition, *Vacuum* 148 (2018) 158–167.